CHALMERS

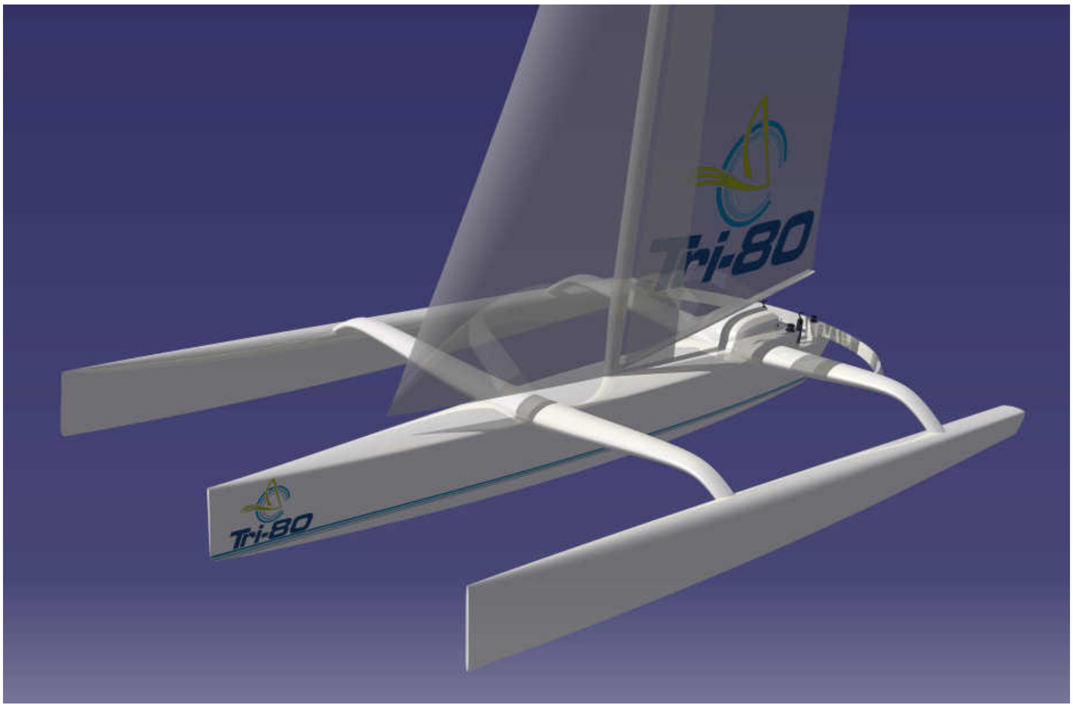

Structural analysis of a multihull racing boat

Master of Science Thesis

BENOIT GAUTIER

Department of Shipping and Marine Technology
Division of Ship Design and Engineering
CHALMERS UNIVERSITY OF TECHNOLOGY
Göteborg, Sweden, 2007
Report No. X-07/213

A THESIS FOR THE DEGREE OF MASTER OF SCIENCE

Structural analysis of a multihull racing boat

BENOIT GAUTIER

Department of Shipping and Marine Technology
CHALMERS UNIVERSITY OF TECHNOLOGY
Göteborg, Sweden 2007

Structural analysis of a multihull racing boat

BENOIT GAUTIER

Report No. X-07/213

Department of Shipping and Marine Technology
Chalmers University of Technology
SE-412 96 Göteborg
Sweden
Telephone +46 (0)31-772 1000

Printed by Chalmers Reproservice
Göteborg, Sweden, 2007

Structural analysis of a multihull racing boat
BENOIT GAUTIER

Department of Shipping and Marine Technology
Chalmers University of Technology

ABSTRACT

In the sailing world, multihulls are presented as the sea formula one sailing boats. They are the most developed racing boat and allow for very high performance in sea. To ensure the structural resistance, the reliability and to improve the racing performance, virtual models are made using the finite element method which is used for structural analysis and development of the products.

This thesis work was part of the development and analysis of a multihull racing boat at the Tri80 design office in France. The project was lead by Mr Yves Parlier who is world-famous for his experience as a sailor and ship designer. The first part of the thesis work was to propose and take part in mechanical testing of composite material specimens used for determination of the mechanical properties of the composite structures used in the multihull structure. In the second part, the establishment of a global FE model of the multihull racing boat was developed considering various scantling distances. The development of a global FE model of the multihull is presented which has been created in the commercial software CATIA. A benchmark between two FE solvers, CATIA and NASTRAN, is presented on a simple composite material specimen. The conclusion from this study was that both softwares could be used for the structural analysis of the multihull structure. Detailed elastic FE calculations are presented on the float structure using three swell load cases, which represent the worst wave load situations the structure is expected to be subjected to during sailing conditions in a race, and two different structure design alternatives with respect to scantling distance. The conclusion was that optimised scantling distance and unidirectional fibre reinforcement on strategic positions in some connections give the structural characteristics as the designers of the mainhull structure anticipated.

The FE calculations reported in the thesis have been carried out using anticipated material data for a similar composite material and fibre orientation. The reason was that the mechanical tests that were planned to be carried out were not completed during the current investigation. Hence, future work should carry out the necessary FE calculations again, using the material data obtained from the testing, to verify that the current investigation's conclusions are still valid.

Keys words: Finite element analysis, composite materials, mechanical testing, multihull racing boat.

PREFACE

This thesis is a part of the requirements for the master's degree at Chalmers University of Technology, Göteborg, and has been carried out from the first of June 2006 to the 31st of October 2006 at the Tri80 design office in Arcachon, France.

I would like to acknowledge Mr Yves Parlier for his interest in the development of my thesis work. He was always there to advice and to support me during these five months**.**

My greetings are going to my examiner and supervisor Associate Professor Jonas Ringsberg at the Department of Shipping and Marine Technology, Chalmers, for his guidance and support. I would also like to thank Remy Gueritte and the Tri80 design office for their concern about my thesis work, for always answering my questions and for making the five months at the office such a nice pleasure.

Many thanks also to my family for their moral and financial support.

Caen, October 2007
Benoît Gautier

CONTENTS

1. INTRODUCTION

1.1. BACKGROUND

In the sailing world, multihulls are presented as the sea formula one racing boats. They are the most developed racing boats and allow for very high performance in sea [1]. The background to this thesis work comes from an idea from the world famous sailor Yves Parlier to build 80 feet multihull racing boats which all should participate in the same sailing competition. The boats should be able to be sailed by a crew of six persons during short races or transatlantic races around the world. Additionally, a multihull racing boat should be able to sail around the world without pit-stop, and of course have good structural resistance for safe sailing in high sea.

This thesis work has been carried out at the Tri80 design office where Yves Parlier is active. He combined a team of experts, called the Tri80 pilot project, which together should design a multihull racing boat. The current thesis was part of that work and carried out the structural calculation analyses of essential parts of the racing boat. Figure 1 shows an example of a multihull racing boat drawn at the French design office *Van Pethegem – Lauriot Prevost*. The dimensions of this boat is length over all (LOA) = 24 m, beam length = 16 m, sail area (upwind) = 334 m^2, draft = 4.5 m and height = 32 m.

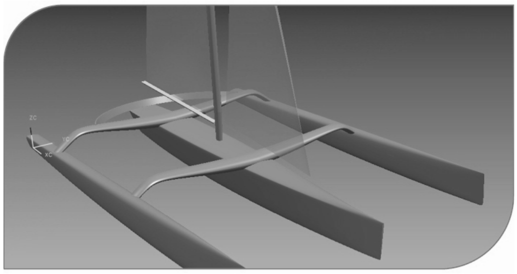

Fig. 1: Example of a multihull racing boat.

Typically, a multihull racing boat is made of composite materials manufactured according to a pre-impregnation fibre process. The hulls and arms have sandwich construction made of a combination of carbon, epoxy and core [1]. The partitions have nomex core instead of the usually used foam. Within the Tri80 pilot project, a semi-industrial production was selected for manufacturing. Hence, the racing boat was divided into main hull, floats, arms, keel and rudder.

1.2. OBJECTIVE WITH THE INVESTIGATION

A design office that works with a new boat project divides the project into several tasks. The objective with the current thesis work was to support and take part of the design and development of the Tri80 pilot project at the Tri80 design office. The tasks reported in this thesis are concerned with the analysis and selection of composite material that makes the multihull, and also to have an active role in the structural analysis of the Tri80 multihull.

The latter task requires expert knowledge, and hence, this work was carried out together with a professional design office called *HDS*, and a technological partner to the Tri80 project called *Dassault* who provided the project with CAD models of the multihull racing boat.

At the start of the project, the intention was to follow the project to its end. Because the Tri80 project ran out of funding, the global structural calculation and analysis of the entire multihull could not be carried out. Consequently, only the completed work and tasks of the project are reported in the thesis: selection of composite material of the multihull, analysis and optimization of the float, and mesh generation and assembling all of the meshed parts of the structure to a completed finite element (FE) model.

1.3. METHODOLOGY

Material testing was carried out to determine the mechanical properties of the composite materials that may be used in the Tri80 multihull boat. A procedure which enables the definition and implementation of material characteristics, obtained from the material testing, in the calculation softwares used was developed.

The commercial software and CAD program CATIA [2] was used to develop the geometry models of the multihull structure. Two FE solvers were compared in a benchmark study on a composite laminate sandwhich structure: the CATIA and MSC NASTRAN [3] softwares. The CATIA software was used for detailed structural analysis of the floats of the multihull racing boat.

2. EXPERIMENTS AND MECHANICAL TESTING

Mechanical tests give mechanicals properties of the materials [4]. Suppliers of composite materials and fibres have often only general material characteristics of their materials which may not be sufficient for more detailed structural calculations. Consequently, experiments were carried out for determination of the mechanical properties of the materials that were of interest for the numerical investigation in this thesis.

2.1. SELECTION OF MATERIAL AND FABRICATION PROCESS

The choice of material for the Tri80 project had to be decided from both an economical as well as a technical point of view. The characteristics of the materials selected must be high resistance and elastic modulus of the composite fibres. Different lamination processes were compared, for example, the infusion and the pre-impregnation fibre processes, and it was decided to emphasise on the pre-impregnated fibre process due to sufficient quality in manufacturing and being a cheaper option as compared with the infusion fibre process [4].

The pre-impregnation fibre process (PrePreg) is today the most used fibre-reinforcement process of composite materials at French shipyard industry for racing boats [1]. PrePreg means that resin is sprayed on the fibres during the manufacturing process of the fabric. During the cure of the new part, the resin will flow and impregnate the fibres. This industrial process gives an optimal fraction between fibres and resin. In a composite laminate, the resistance is determined by the fibres and their orientation. The process is known for its high quality and mechanical characteristics of the laminated composites [5].

Two PrePreg systems with different temperature of reticulation is available on the composite market: the high temperature system, above 120°C, and the low temperature system, which is up to maximum 80°C and requires a longer curing time (about 15h) in contrast to the former system. The Tri80 project selected the low temperature PrePreg system justified by the lower cost. In addition to the low temperature PrePreg system, another alternative referred to as the SPRINT manufacturing technology was also investigated by the project. SPRINT is a new composite manufacturing process technology developed by the *Gurit Composites Group*. Mechanical test results and low cost of the composite materials motivated a comparison between the SPRINT and PrePreg systems.

2.1.1. THE LOW TEMPERATURE PREPREG PROCESS

A PrePreg fabric is made of a dry fibre that is impregnated with resin, see Fig. 2 for a schematic description. Impregnation rates are controlled by the supplier and can be adapted. The different PrePreg laminate skins are deposed in a mould, whereafter the mould is cured in an oven to obtain the desired rigidity and resistance of the composite material [6].

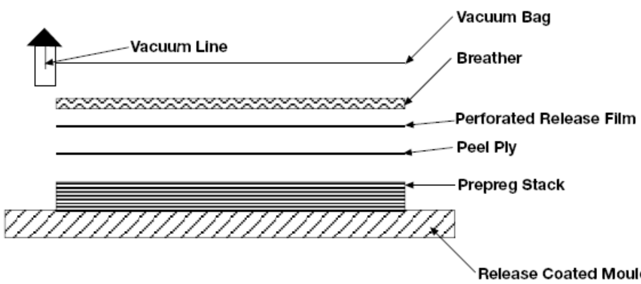

Fig. 2: Illustration of PrePreg laminate skins [6].

Table 1 lists the advantages and disadvantages of the low temperature PrePreg process composite material.

Table 1: Advantages and disadvantages of the low temperature PrePreg process.

Advantages	Disadvantages
• Accepted and well-known by shipyards • Easy to access for a shipyard • Low cost of tooling • Wide selection of core materials • Fairly low energy consumption in the manufacturing process (oven)	• Price may be too high for the materials • Fairly long manufacturing process • High labour price in the manufacturing process

2.1.2. THE SPRINT PROCESS

SPRINT is a technology developed by the Gurit Composites Group and it is the abbreviation for SP Resin Infusion Transfert. This new technology is a combination of the infusion and low temperature PrePreg processes. The fibres and the core are placed in the mould similar to the infusion process. Curing can be done in "one shot" (all the plies and core catalysed at the same time). But contrary to the infusion process, the SPRINT process can easily quantify and control the impregnation rates of the fibres [6].

Table 2 lists the advantages and disadvantages of the SPRINT manufacturing process of laminated composite material.

Table 2: Advantages and disadvantages of the SPRINT manufacturing process.

Advantages	Disadvantages
• Simple and well-controlled method • Fast and reliable process • Result show excellent mechanical properties (resistance and strength) • Less than 1% porosity in the final product • Fairly low price on the final product	• Unknown materials at French shipyards • New materials which are still in their development process.

In Fig. 3, the pictures show examples of large luxury yachts which have been built by composite material using the SPRINT technology.

Fig. 3: Pictures of luxury yachts built with the SPRINT composite material technology [6].

2.2. SUPPLIERS OF COMPOSITE MATERIALS

Three suppliers of PrePreg fibres in Europe were contacted: *SP systems* (Gurit in the U.K), *Hexcell* (France) and *Structil* (France). SP systems could also supply the Tri80 project with the SPRINT technology for comparison.

- SP systems was the core supplier of material to the project, and the foam Corecell P500 was selected. It is a foam with high strength properties with good impact resistance. It is advised to be used for fabrication of sandwich laminate structures with curing at low temperature (below 85°C).
- Hexcel and Structil supplied the Tri80 project with a resin called Epoxy M10.

2.3. TEST PLAN FOR THE MECHANICAL TESTING

The mechanical tests were carried out using normalised test bars manufactured by the team at the Tri80 design office. Five test bars for each test and each material were manufactured. To types of tests were carried out, see Tables 3 and 4: one range in monolithic carbon and the other range in sandwich carbon-foam. Monolithic carbon means that all of the plies have the same direction, i.e. unidirectional fibres were used in these specimens. Sandwich carbon means that different carbon fibre directions were used in these specimens; see BBC and EQC in Fig. 20.

The monolithic test bars had a normalized thickness of 1.8 to 2.0 mm. The sandwich laminate test bars were manufactured considering the general scantling plans provided by the multihull racing boat architects. The scantling used in the tests were taken in the main hull plating between the two link arms, where large stresses are expected to occur when sailing at sea. The thickness of the sandwich test bars was approximately 25 mm.

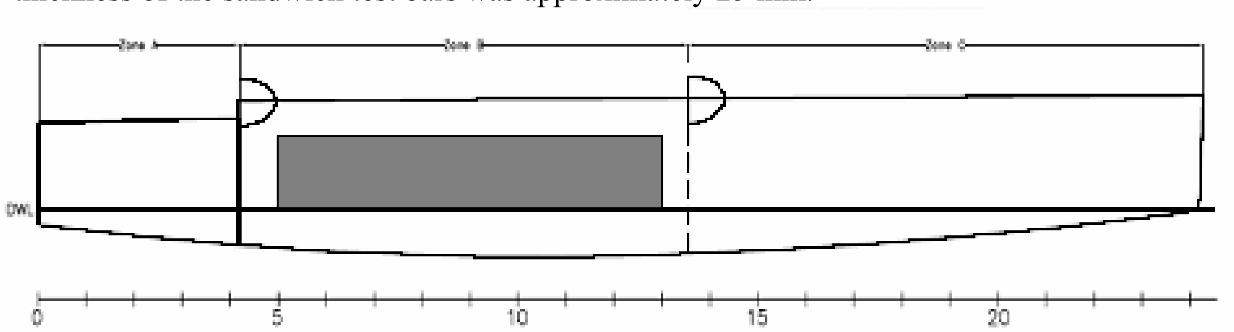

Fig. 4: Side view of the main hull for localisation of the scantling.

Table 3: Tests with monolithic tubes [4].

Tests	Specimen size L×W(mm)	Scantling – thickness	Objective with test
• Tensile testing	• 250×50	• 6 plies, t=1.92 mm	• Tensile properties of unidirectional fibres
• Three-point bending test	• 100×10	• 6 plies, t=1.92 mm	• Modulus of rupture in bending
• Short normalised bending test	• 20×10	• 6 plies, t=1.92 mm	• Shear failure of the laminate
• Porosity test using an optical method	• -		• Quantification of the porosity rate in the laminate

Table 4: Tests with sandwich laminated tubes [4].

Tests	Specimen size L×W (mm)	Scantling – thickness*	Objective with test
• Three-point bending test	• 600×100	• 3BBC+1EQC+P500 (t = 25mm)	• Shear fracture of the foam in the laminate
• Four-point bending test	• 600×100	• 3BBC+1EQC+P500 (t = 25mm)	• Ply resistance of sandwich laminate in wrinckling
• Wrinckling test	• 150×100	• 3BBC+1EQC+P500 (t = 25mm)	• Sandwich plies buckling and wrinckling modulus
• Transverse tension test	• 50×50	• 3BBC+1EQC+P500 (t = 25mm)	• Bonding between plies and foam
• Impact test	• 150×100	• 3BBC+1EQC+P500 (t = 25mm)	• Sandwich laminate resistance during impact

* See Fig. 20 for the definition of BBC, EQC and P500.

2.4. PREPARATION AND MANUFACTURING OF TEST SPECIMENS

The fibres were cut to dimensions 450x500 mm. The size was determined by the size of the oven. To facilitate the mitigation of resin in the core, small holes were drilled in the foam over its the entire area, see Fig. 5. The fibres were put in layers on the foam and cured with aluminium panel sup in the oven during 14 h 20 min at a maximum temperature of 90°C.

Fig. 5: Preparation of specimens – hole drilling in the foam.

The panels were cut to bar specimens using a jigsaw with a special type of diamond blade; see Fig. 6 for cut specimens.

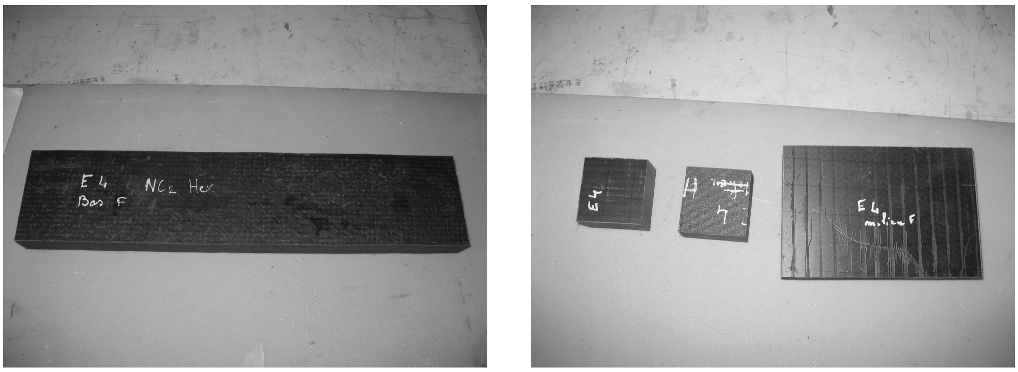

Fig. 6: Specimens cut from panels.

2.5. MATERIAL AND MECHANICAL TESTING

The material testing presented in Table 4 was carried out at the mechanical laboratory *LAMEFIP* in Bordeaux which is the material laboratory of *l'Ecole Nationale Supérieure des Arts et Métiers de Bordeaux*. In addition, during this thesis work only three of the planned material and mechanical tests were completed: the three-point bending test, the four-point bending test and the wrinkling test. In all of these tests, the loading rate was 1 mm/min. Figure 7 to 9 present the material curves and data from the tests.

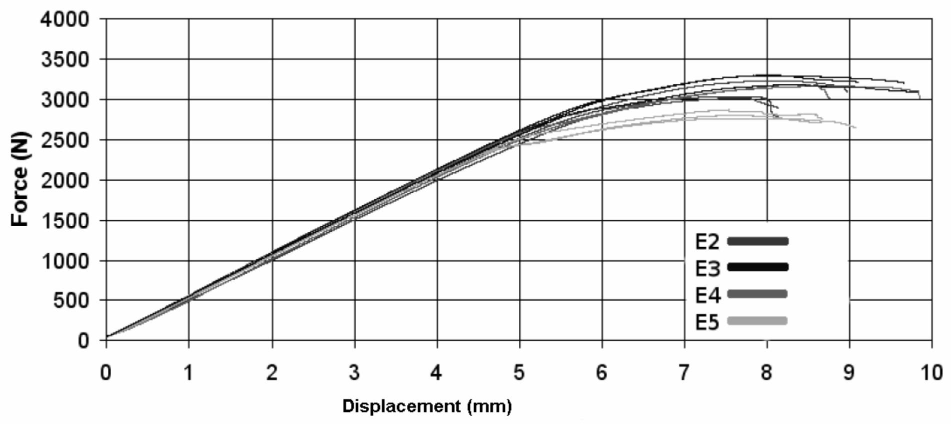

Test	Stiffness: mean±stdv (N/mm)	Peak force: mean±stdv (N)
E2	508 ± 17	3092 ± 118
E3	520 ± 7	3257 ± 63
E4	514 ± 8	3176 ± 10
E5	514 ± 2	2809 ± 54

Fig. 7: Results from the three-point bending tests.

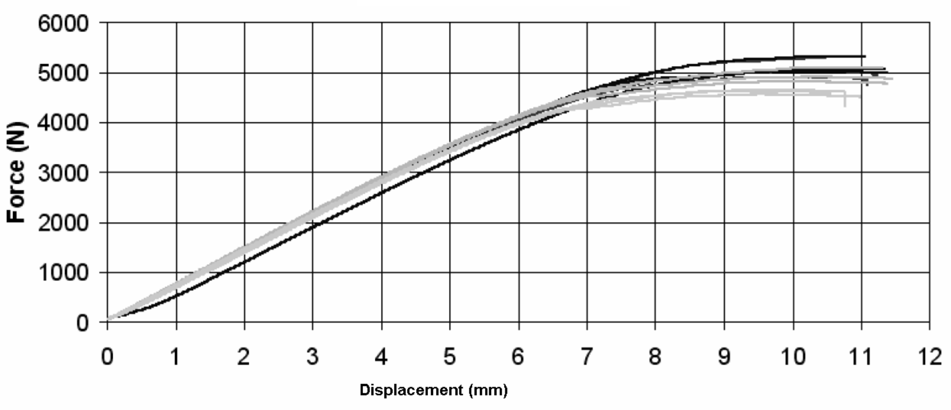

Test	Stiffness: mean±stdv (N/mm)	Peak force: mean±stdv (N)
E2	698 ± 4	5081 ± 215
E3	693 ± 22	5134 ± 165
E4	711 ± 2	4938 ± 139
E5	694 ± 6	4605 ± 49

Fig. 8: Results from the four-point bending tests.

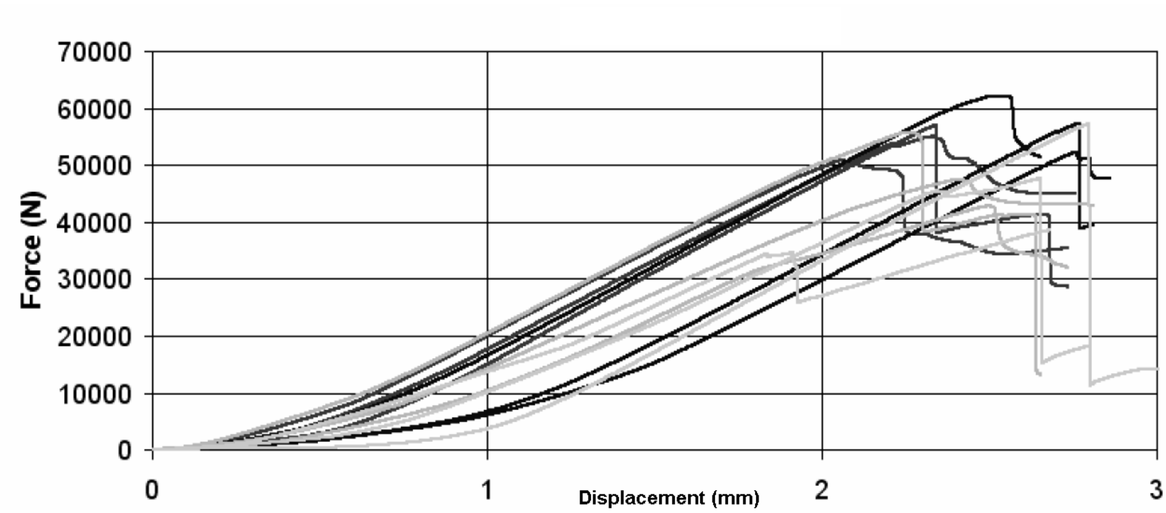

Test	Stiffness: mean±stdv (N/mm)	Peak force: mean±stdv (N)
E2	31140 ± 990	54309 ± 3089
E3	29315 ± 2587	57648 ± 4256
E4	27488 ± 2782	48629 ± 6555
E5	26816 ± 5087	48479 ± 8287

Fig. 9: Results from the wrinckling test.

The wrinckling tests showed larger scatter in results in comparison with the other tests. An examination of the test specimens showed that the thickness of the specimens were not uniform. It was observed that, during the curing process, the vacuum bag compressed the corner of the upper side of the specimens, which created a non-uniform thickness with a thinner section near (some of) the sides of the specimens.

3. NUMERICAL ANALYSES OF SMALL COMPOSITE PANELS

The main function of the fibres in a composite is to carry the loads. In a structural composite, 70 to 90% of the load is carried by the fibres which also to contribute to stiffness, strength, thermal stability and other structural properties of the composites. In addition, the material representation of composite materials characteristics in a FE code is considered using an orthotropic material description. The reason is that the composite fibres are laminated in the moulds in various directions, i.e. each ply of carbon does not have the same direction. The orientation of the fibres and the number of layers determines the characteristics of the composite structure.

In the Tri80 project, the fibres were oriented in four directions in the different layers: 0°, 45°, -45° and 90°; see Fig. 10. Here, 0° is in the *x*-direction which is in the longitudinal direction of the multihull drawing, and 90° is in the *y*-direction which corresponds with the transverse direction of the multihull.

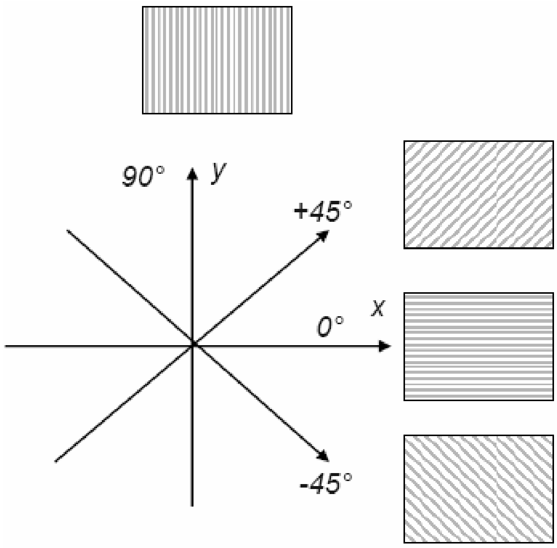

Fig. 10: Illustration of fibre orientations in the composite material.

The ply layers are numbered from one to the number of layers that define the composite panel. For the monolithic panel, a line of symmetry where the FE mesh is positioned is put in the middle of the number of plies, while for the sandwich composite the symmetry plane is put in the middle of the foam, see Fig. 11.

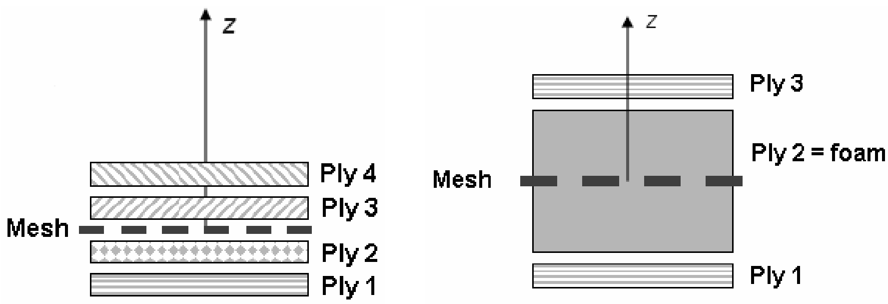

Fig. 11: Illustration of mesh symmetry line for the monolithic and the sandwich composite panels.

3.1. CALCULATION SOFTWARES AND COMPOSITE CHARACTERISTICS

The geometry design and modelling of the multihull racing boat was carried out using the commercial software CATIA ver 5. Using this software, it is also possible to carry out finite element calculations using one of the modules in the software. For comparison, the commercial FE software called NASTRAN was also used. A benchmark was made between the two FE solvers, see Section 3.2, to investigate which of the softwares that was going to be used in the structural analysis of the entire multihull structure and its parts.

This section describes the representation of the composite material and its characteristics in CATIA. To enable realistic modelling and representation of composite materials, the following information has to be defined [7]:

- type of material in the fibres (carbon, kevlar or glass fibre),
- thickness of a ply,
- fibre orientation and
- position of the plies and fibres in the laminate scantling.

Because this information cannot be specified in the CATIA software, the composite material characteristics had to be imported to CATIA from another program using an XML-file interface which specifies the necessary characteristics. The XML-file connects a laminate scantling to each part of the mesh of the structure. An example of a XML-file used for the composite panel and its scantlings used in Section 4 is presented in Fig. 12.

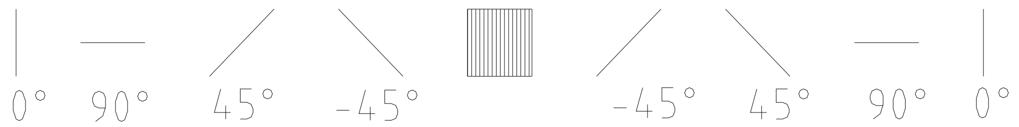


```
  <?xml version="1.0" encoding="UTF-8" ?>
-<ListOfProperties xmlns:xsi="http://www.w3.org/2001/XMLSchema-instance"
     xsi:noNamespaceSchemaLocation="PropertyMappingRules.xsd">
  <DEFAULT_VALUES TOL="0.001" AXIS="0;0;0;1;0;0;0;1;0" />
  <UNITS LENGTH="mm" ANGLE="deg" />
-<COMPOSITE_SHELL BELONG_TO_MP="Maillage plaque" COMPOSITE_AXIS="Axis
     Systems\rep1">
  <LAMINA MAT="Carbone UD HR" TH="0,162" ANGLE="0" POSITION="9" />
  <LAMINA MAT="Carbone UD HR" TH="0,162" ANGLE="90" POSITION="8" />
  <LAMINA MAT="Carbone UD HR" TH="0,162" ANGLE="45" POSITION="7" />
  <LAMINA MAT="Carbone UD HR" TH="0,162" ANGLE="-45" POSITION="6" />
  <LAMINA MAT="Mousse H80" TH="20" ANGLE="0" POSITION="5" />
  <LAMINA MAT="Carbone UD HR" TH="0,162" ANGLE="-45" POSITION="4" />
  <LAMINA MAT="Carbone UD HR" TH="0,162" ANGLE="45" POSITION="3" />
  <LAMINA MAT="Carbone UD HR" TH="0,162" ANGLE="90" POSITION="2" />
  <LAMINA MAT="Carbone UD HR" TH="0,162" ANGLE="0" POSITION="1" />
    </COMPOSITE_SHELL>
    </ListOfProperties>
```


Fig. 12: Example of a XML file for the scantling of the composite panel studied in Section 4.

A short description of the information in the XML-file lines is given below:

- **Lines 1 – 5:** definition of units, angles and setup common for XML files.
- **Lines 6 – 7:** matches the meshed geometrical surface and the coordinate system axis with the material library orientations in the CATIA software.
- **Lines 8 – 16:** definition of the laminate sequences of the panel. In the current example, all of the plies are defined as carbon UD HR (unidirectional and high resistance carbon fibres), with 1.62 mm thickness. The first ply is in position #1 followed by #2 to #4 until #5 defines the foam. Thereafter #6 to #9 follows in accordance with Fig. 12. The plies have different angles as specified in Fig. 12: 0°, 90°, -45° and 45°.
- **Lines 17 – 18:** ends the XML-file.

3.2. FE ANALYSIS OF A SMALL COMPOSITE SANDWICH LAMINATE PANEL

In this section, a numerical comparison of the CATIA and NASTRAN FE solvers is presented. The objective with the comparison of softwares was to:

- compare the results from CATIA with the results from NASTRAN and
- to study the compatibility between CATIA and NASTRAN with respect to mesh and material properties exported from CATIA to NASTRAN.

One of the reasons for this comparison was that a partner in the Tri80 project used the NASTRAN software while the Tri80 design office prefers the CATIA software. In addition, the FE analysis was carried out on a small composite sandwich laminate panel loaded with a uniform surface pressure. The length of the panel was 1000 mm and its width was 500 mm. Quadratic shell elements with linear integration made the mesh and convergence analysis resulted in the mesh size approximately 15×15 mm. The boundary conditions along the edges were fixed, i.e. no translations or rotations, and the magnitude of the uniform surface pressure was 0.01 MPa to achieve elastic response. In addition, the composite sandwich laminate characteristics were represented using the same example that was presented in Section 3.1, using the material properties presented in Table 5. Those values are "typical" values for the current materials (note: they are not taken from the experiments presented in Section 2).

Table 5: Material properties: fibres and plies in small composite laminate sandwich panel [6].

Fibre	**carbon HR**	**mousse H80**
Ply	**UD**	**R63-80**
Longitudinal Young's modulus	115100 MPa	50 MPa
Transversal Young's modulus	5140 MPa	50 MPa
Poisson's ratio	0.3	0.3
Shear modulus in XZ plane	2500 MPa	21 MPa
Shear modulus in XZ plane	2500 MPa	21 MPa
Shear modulus in YZ plane	2500 MPa	21 MPa
Density	1500 kg/m^3	80 kg/m^3
Ply thickness	0.162 mm	20 mm
Longitudinal tension constraint	1200 MPa	1.4 MPa
Longitudinal strain constraint	1000 MPa	1.4 MPa
Transverse tension constraint	50 MPa	1.4 MPa
Transverse strain constraint	100 MPa	1.4 MPa

The following results were compared between the CATIA and NASTRAN FE calculations; see Fig. 13 for definition of the coordinate system axis and Table 6 for the results:

- The vertical displacement (z-direction) of the panel under the pressure load.
- The stress in the ply with fibre orientation 0°.
- The stress in the ply with fibre orientation 90°.
- The stress in the bidirectional ply with fibre orientations 45° and -45°.
- The shear stresses τ_{xz} and τ_{yz} in the foam.

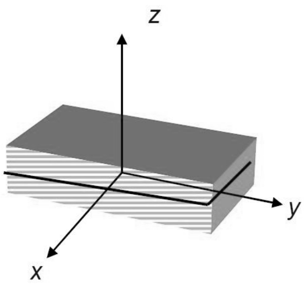

Fig. 13: Definition of the coordinate system axis of the composite sandwich laminate panel.

Table 6: Results from the FE analyses of the small composite laminate sandwich panel.

FE analysis result	**CATIA**	**NASTRAN**
Max displacement	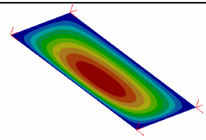 1.74 mm	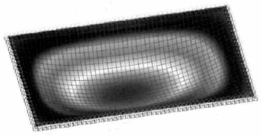 1.42 mm
Stress in 0° ply	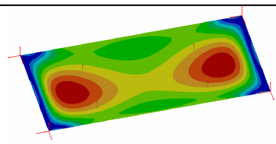 14.5 MPa	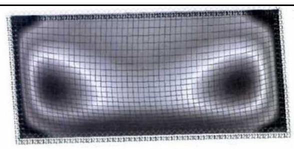 14.6 MPa
Stress in 90° ply	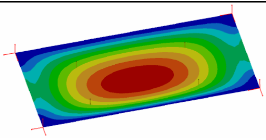 48.6 MPa	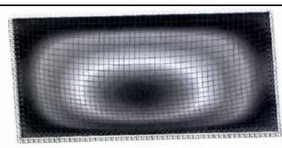 48.3 MPa
Stress in bidirectional ply	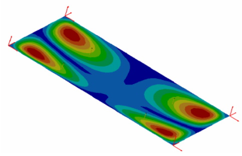 7.4 MPa	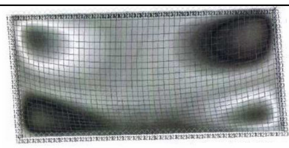 8.6 MPa
XZ shear stress in the foam	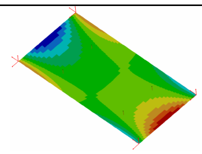 0.09 MPa	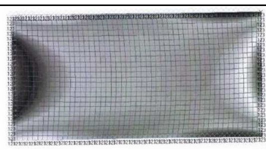 0.09 MPa
YZ shear stress in the foam	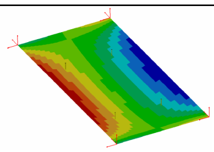 0.12 MPa	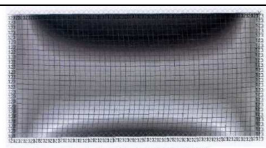 0.12 MPa

The results presented in Table 6 show good agreement between softwares except for the panel displacement and the shear stress in the biaxial ply. The discrepancies in these two results were not related to model representation. Instead, it was due to different interpretation of the softwares how these values should be presented (reference coordinate systems: local or global). A recalculation of the values using the same definition from both softwares resulted in good agreement in results. Consequently, for the current investigation and future FE calculations, either CATIA or NASTRAN can be used for this type of structural analysis calculations. Furthermore, for a more thorough comparison between FE softwares, it is recommended to compare calculation results using a more complicated geometric shape with curves and edges that are more similar to the Tri80 multihull design.

4. ESTABLISHMENT OF GLOBAL MULTIHULL GEOMETRY MODEL

This section presents the design and development of the global multihull geometry in the CATIA software. The drawings of the Tri80 multihull boat were followed in detail for each of the major parts of the structure: main hull, floats, arms and traveller track; see Fig. 14.

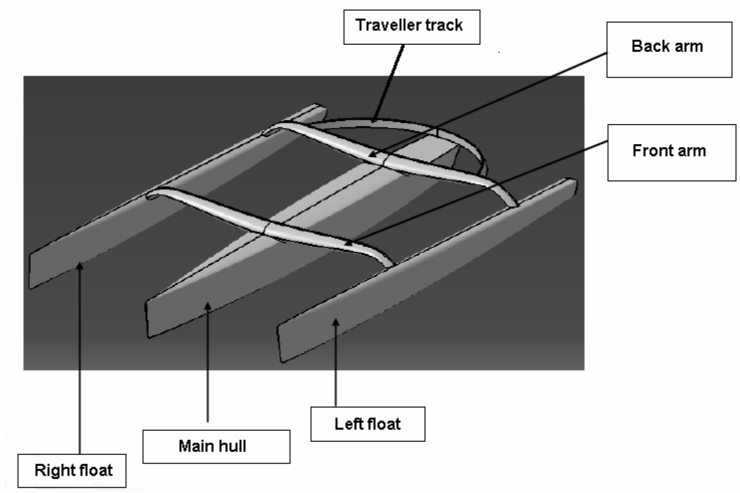

Fig. 14: Definition of the major parts included in the global geometry model of the multihull.

The global geometry model was divided into a large number of surfaces which was going to be attributed to different characteristics in the detailed modelling and finite element mesh procedure, see Section 5 for the floats. Thus, the interior structural parts illustrated in Fig. 15 were considered and modelled in a later stage of the multihull model development process.

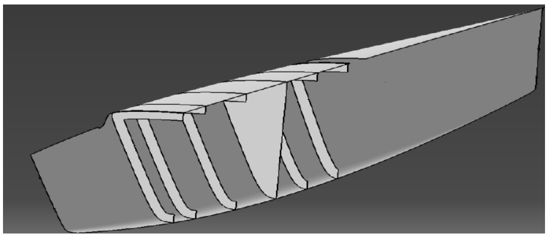

Fig. 15: Example of interior structural parts that are modelled in a later stage of the complete multihull geometry model.

To check that the global geometry model and all its parts were properly attached to each other, an eigenmode analysis was carried out. In order to do that, the geometry model was automatically meshed in CATIA using quadratic shell elements. Figure 16 shows the finite element mesh created for one half of the model.

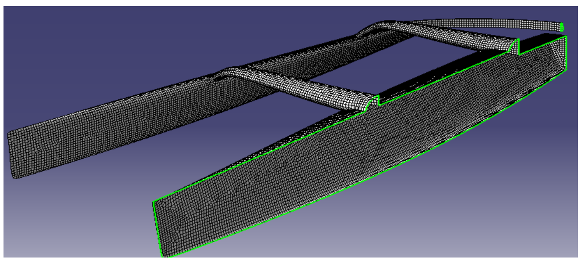

Fig. 16: Finite element mesh of one half of the global geometry model.

In the FE analysis, the displacements and rotations of the back panel and the first bulkhead (limited by the crash box) of the main hull were fully restrained (fixed). The material of the structure was given the properties of a typical aluminium material with sheet panel thickness 3 mm. In addition, the FE analysis calculated the three first eigenmodes. The results showed that all of the parts were properly connected to each other. Figure 17 shows the first eigenmode calculated by the FE analysis [7].

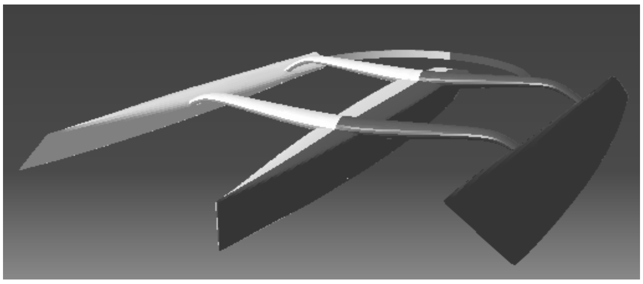

Fig. 17: The shape of the first eigenmode of the global hull geometry using an aluminium material description of the structure.

5. STRUCTURAL ANALYSIS OF THE FLOATS

This section presents a detailed analysis of the floats using FE calculations of various load cases. It was decided to start with detailed structural analysis of the floats because their geometry and composite laminate scantling was not as detailed and complicated as the main hull part. In Section 5.1, the detailed geometry model of a float is presented. The FE mesh generation using the geometry model is presented in Section 5.2 followed by structural analysis calculations for various load cases in Section 5.3.

5.1. DESCRIPTION OF FLOAT GEOMETRY MODEL

One of the floats' surface geometry were extracted from the global geometry model, see Fig. 18. This surface geometry model has no interior structural frame, hence, it has to be modelled. The entire bulkhead and floor panel geometries were modelled in accordance with the drawings made by the designers and the architects of the mutihull boat. The bulkhead and floor panels were created as surface elements without thickness and material properties, see Fig. 19. These properties were considered at a later stage in the development of the model.

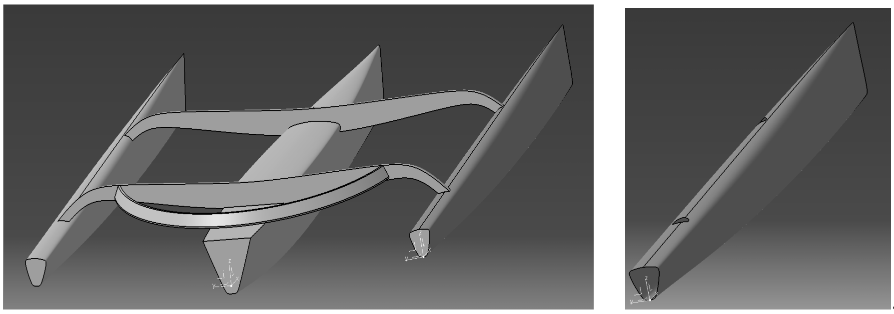

Fig. 18: Extraction of a float surface geometry model.

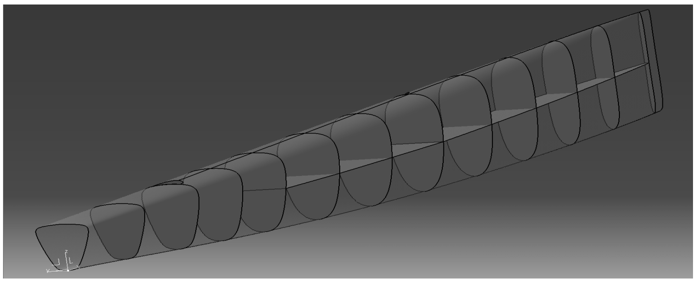

Fig. 19: Float with bulkhead and floor panels.

The composite laminate scantling is not constant but changes with position and area on the float. For example, from the back panel to the middle line of the float, the composite laminate is the same for both deck and hull while the front part planking on the hull is reinforced by one ply of equilibrate layer in order to support pressure from waves. The variation in composite laminate scantling is shown in Fig. 20 and Fig. 21.

Unidirectional fibres are used to reinforce the structure to give improved longitudinal strength of the float. These layers are laminated during the building between the hull's nominal fibres. In Fig. 20, the composite laminate scantling for unidirectional fibres is divided in two studies: homogeneous scantling with 10 plies, and variable unidirectional fibre scantling along the hull in accordance with the architect's design. The two options were compared and evaluated in the structural analysis calculations.

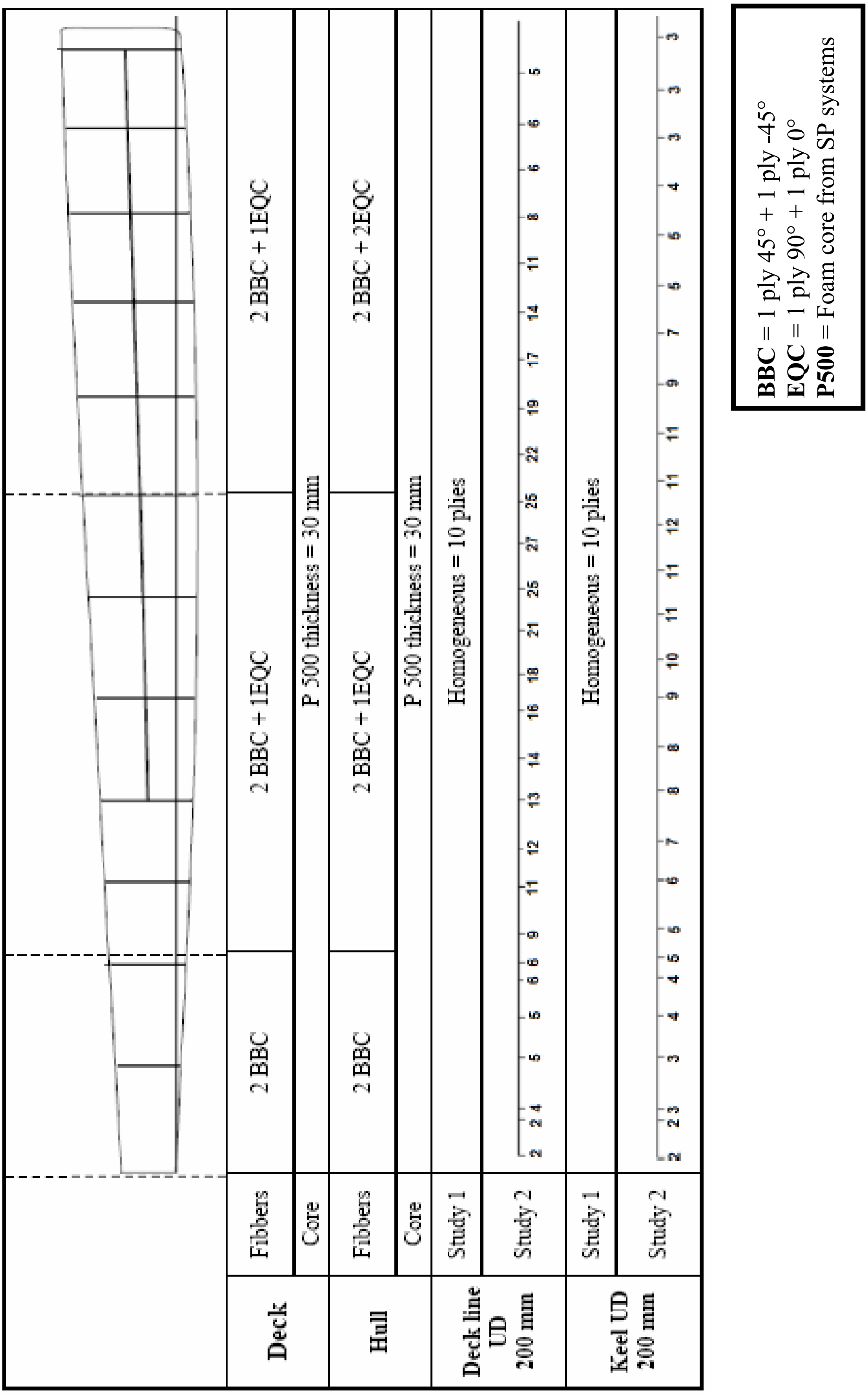

Fig. 20: General scantling of the float and presentation of two scantling studies. The bars show the number of UD carbon plies along the length of the float.

The general arrangement of the composite scantling is illustrated in Fig. 21. The float was divided into five zones where each zone corresponds with unique material properties definitions for the composite scantlings [7]:

- Zone A: back hull and back deck
- Zone B: central hull and central deck
- Zone C: front hull and front deck
- Zone D: port side and starboard deck line UD
- Zone E: keel UD

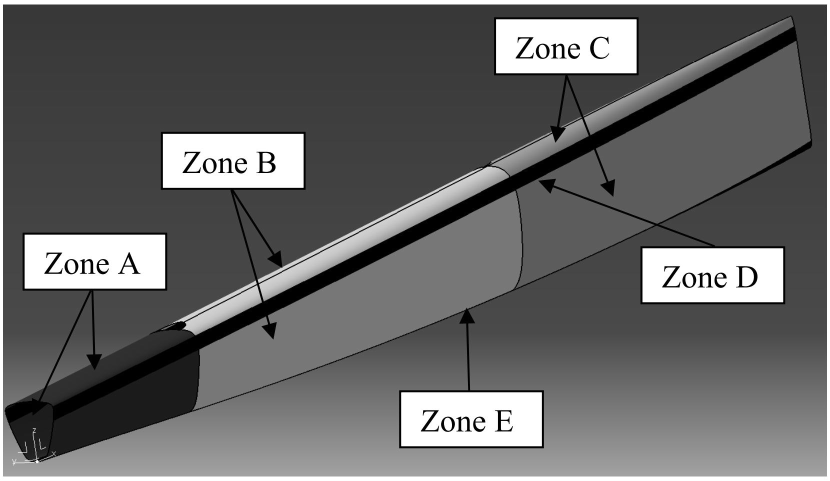

Fig. 21: Definition of float areas zone A - E.

5.2. FINITE ELEMENT MESH

The FE mesh of the float was made of 80 mm quadratic shell elements. This type and size of elements have been used in previous studies by the Tri80 design office team and has shown satisfactory results for similar type of investigations [8].

The FE mesh of the zones D and E was different between study 1 and 2. In study 1, the unidirectional zone was considered as a homogeneous zone, i.e. the number of plies was not changing along the float. Ten UD plies were modelled and meshed in these zones. In study 2, however, the laminate plan proposed by the designers was followed, i.e. the number of UD plies was changing along the float. In Fig. 22, a FE mesh of the float is presented.

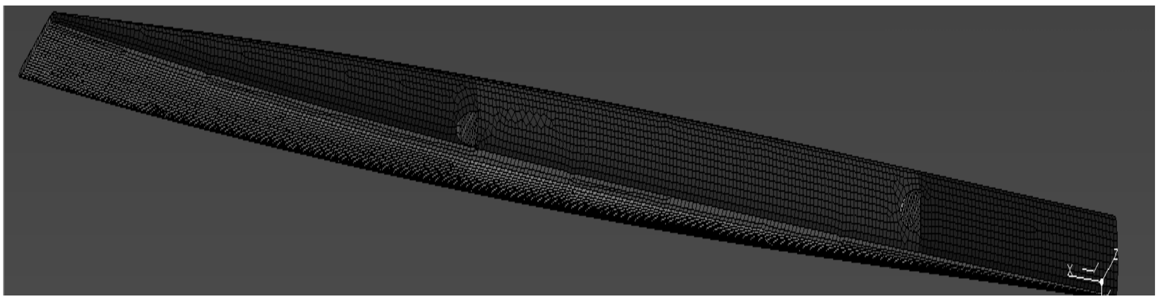

Fig. 22: Finite element mesh of the float.

5.3. STRUCTURAL ANALYSIS CALCULATIONS AND RESULTS

The mechanical properties of the composite material and its components were taken from Table 5 in Section 3.2. Since all of the planned materials testing was not been completed during this thesis work, those values had to be used instead.

The structural analysis calculations were divided into two parts. In the first part, three load cases were compared in order to determine the worst load case the float was subjected to. The composite laminate scantling was represented as described in Section 5.1 for study 1 with standard keel and deck line unidirectional fibre scantling. In the second part of the current section, the worst load case as determined in the former part was applied to the float, now with a composite laminate scantling which followed study 2 and Fig. 20 in Section 5.1. Additionally, a load pressure study on the planking of the float was also made.

5.3.1. STUDY 1 - COMPARISON OF THREE SWELL LOAD CASES

Three different swell loads cases were compared and applied on three different areas of the float. The objective was to determine which of the load cases that resulted in the largest displacement and maximum shear stress in the fibres. This load case was thereafter used in Section 5.3.2 to optimize the scantling of unidirectional fibres in the hull and deck. In addition, there are four outer sources that contribute to stresses in a racing multihull:

- aero-dynamical stresses transmitted by the rig,
- hydrodynamic stresses applied on the floats and the main hull,
- stresses given by the centre-board on the main hull and
- hydrostatic pressure applied on the hull and the arms.

In this investigation, only the hydrodynamic stresses and hydrostatic pressures were applied on the float. The boat displacement, *D*, was assumed to be 10 tonnes and the antidérive force, *FA*, was 5.5 tonnes. The hang-up arms were excluded in the FE model and replaced by restraining boundary conditions at their connections with the float, see Fig. 23.

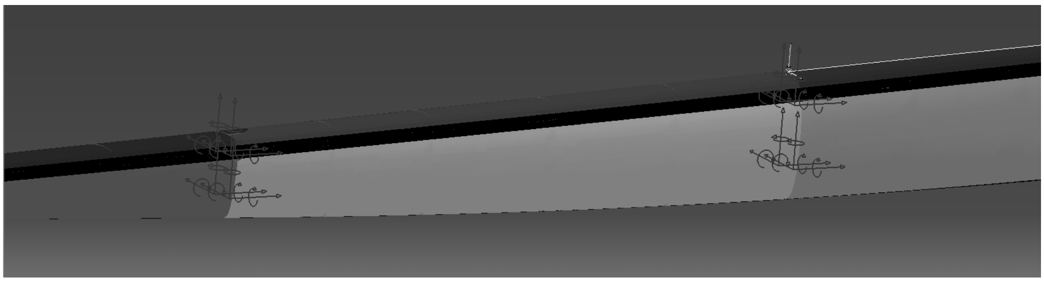

Fig. 23: Boundary conditions that replace the hang-up arms in the FE analysis.

The three swell load cases that were compared are presented in Fig. 24 to 26. They were selected by the HDS structural design office and the Tri80 design team who have many years of experience of multihulls structural designs and analysis.

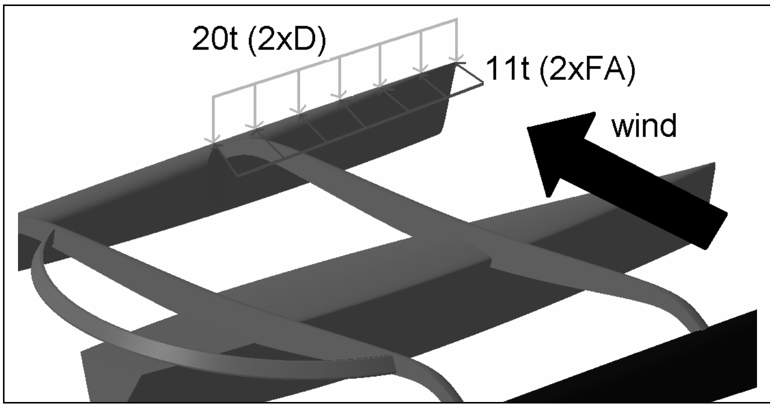

- Load case with yaw of the front of the float.
- The front part of the float under the wind will support the entire Archimede (*D*) and anti-derive forces (*FA*).
- The dynamic coefficient was set to 2 for this load case.

Fig. 24: Swell load case 1: yaw of the front of the float.

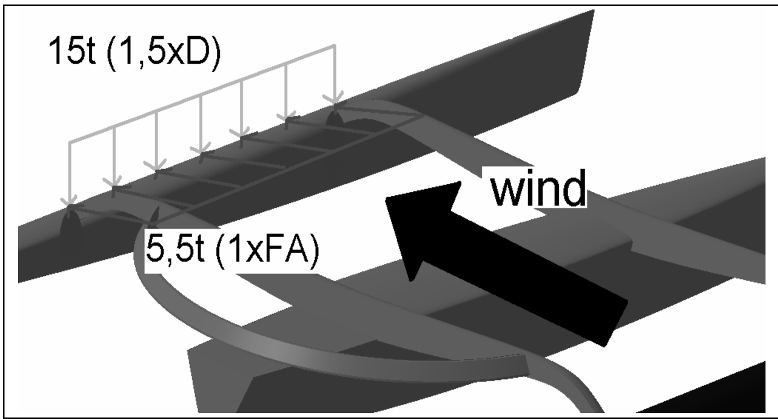

- Load case with waves which are loading the area between the two arms.
- The area located between the two arms supports the entire Archimede and anti-derive forces of the multihull.
- The Archimede force is multiplied by a dynamical coefficient of 1.5.

Fig. 25: Swell load case 2: wave load case between the two hang-up arms.

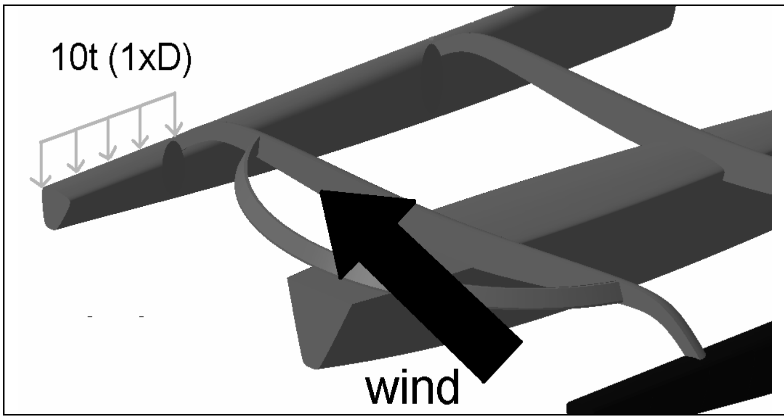

- Load case where waves are loading the back part of the float.
- The back part of the float under the wind just beside the back arm support the entire Archimede force of the multihull.

Fig. 26: Swell load case 3: wave load case in the back part of the float.

The FE calculations were carried out using the software CATIA ver 5. The results from the three load cases were compared with respect to maximum displacement of the float and the maximum shear stress in any part of the float for biaxial and unidirectional fibres. The motivation for study of shear stresses is that for composite materials, shear stresses are the most dangerous stresses with respect to adhesion between layers and fibres because the shear stress values are constant in a ply and will give information regarding its adhesion to the composite part [4].

Swell load case 1: yaw of the front of the float.

Figure 27 presents the calculated displacement of the float for load case 1. The maximum displacement was calculated to 103 mm. Figure 28 shows an example of the principal shear stress for the same load case, and Table 7 presents the principal shear stresses in different parts of the float.

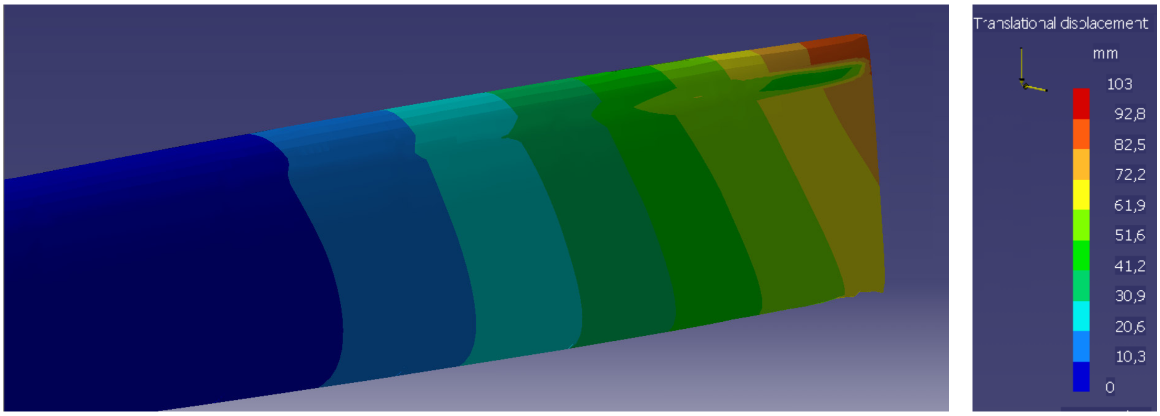

Fig. 27: Calculated displacement of the float for load case 1.

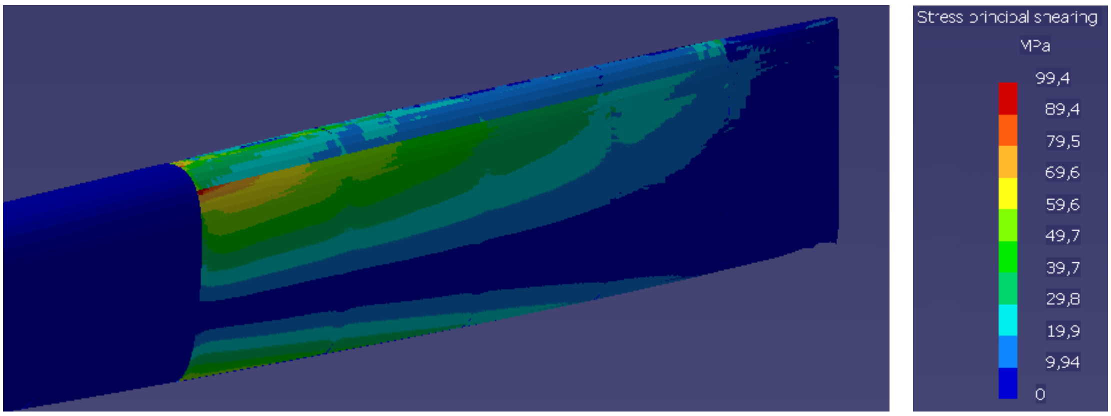

Fig. 28: Example of calculated principal shear stress of the float for load case 1.

Table 7: Summary of calculated principal shear stresses for load case 1.

	Principal shear stress (MPa)	Stress rupture (MPa)	Safety coefficient
Bulkhead biaxial	112	300	2.7
Panel floor biaxial	37	300	8.1
Keel UD	231	1000	4.3
Deck line UD	263	1000	3.8
Deck Biaxal	140	300	2.1
Hull Biaxal	100	300	3.0

Note that the maximum shear stresses are quite similar in the deck, hull and bulkhead with a safety coefficient of three. The results indicate that the float structure can resist a brutal bump in a large wave.

Swell load case 2: wave load case between the two hang-up arms

Figure 29 presents the calculated displacement of the float for load case 2. The maximum displacement was calculated to 2.4 mm. The value is reasonable due to that this part of the float is restrained between the two bulkheads. Figure 30 shows an example of the principal shear stress for the same load case, and Table 8 presents the principal shear stresses in different parts of the float.

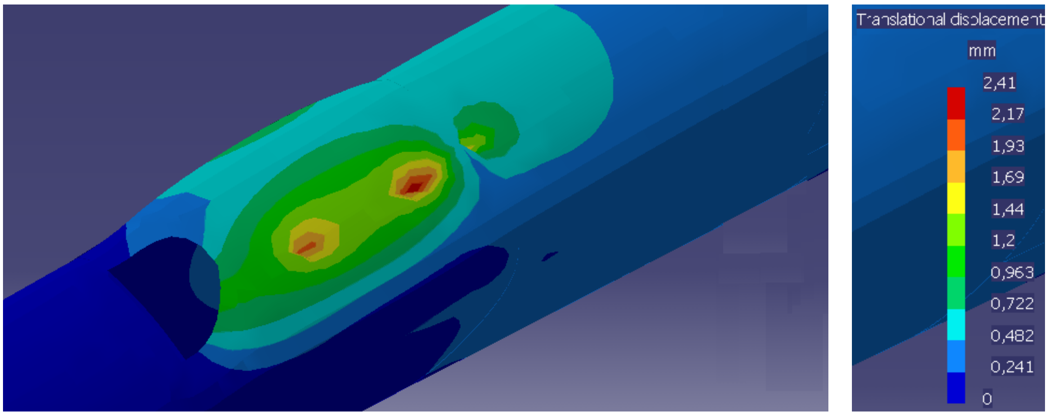

Fig. 29: Calculated displacement of the float for load case 2.

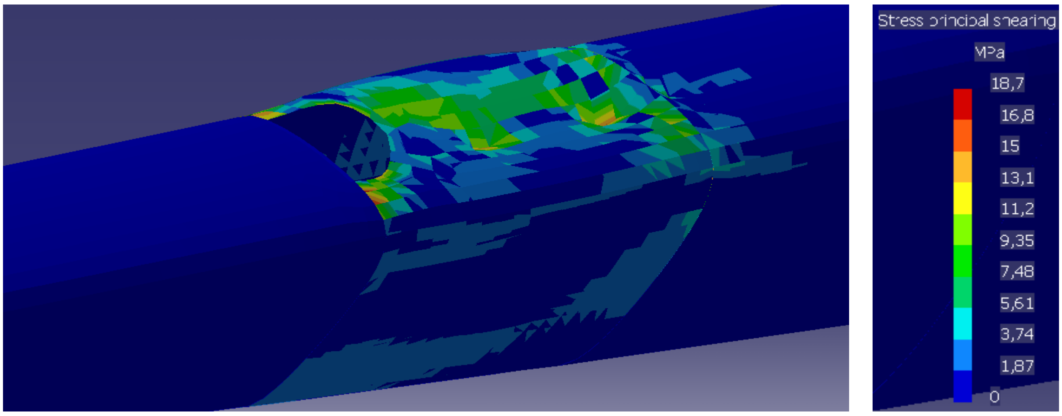

Fig. 30: Example of calculated principal shear stress of the float for load case 2.

Table 8: Summary of calculated principal shear stresses for load case 2.

	Principal shear stress (MPa)	**Stress rupture (MPa)**	**Safety coefficient**
Bulkhead biaxial	17	300	17.6
Panel floor biaxial	1	300	300
Keel UD	5	1000	200
Deck line UD	13	1000	76.9
Deck Biaxal	33	300	9.1
Hull Biaxal	6	300	50

The maximum principal shear stress occurs in the deck and it is approximately 30 MPa. Note that all of the safety coefficients are high for this load case, i.e. no damage caused to the hull is expected for this load case.

Swell load case 3: wave load case in the back part of the float

Figure 31 presents the calculated displacement of the float for load case 3. The maximum displacement was calculated to 2.0 mm. The value is reasonable since the distance between the back panel of the float and the bulkhead is about 4 metres which is not enough to create a large bending moment and displacement. Figure 32 shows an example of the principal shear stress for the same load case, and Table 9 presents the principal shear stresses in different parts of the float.

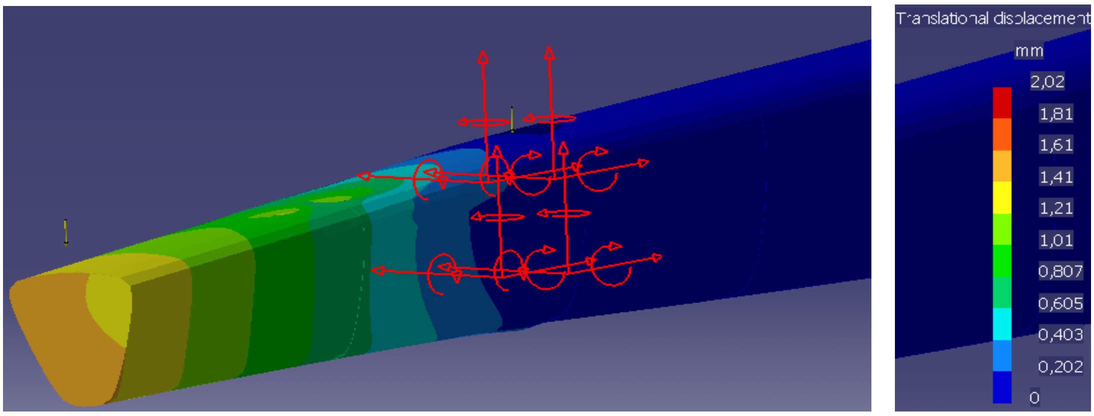

Fig. 31: Calculated displacement of the float for load case 3.

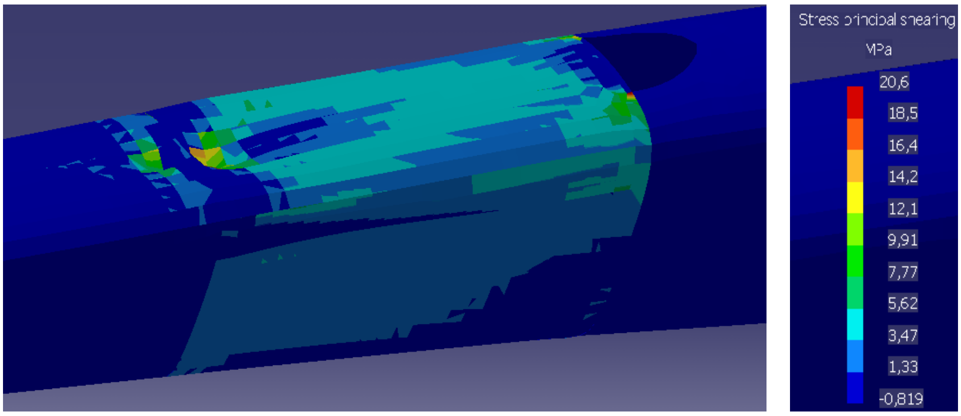

Fig. 32: Example of calculated principal shear stress of the float for load case 3.

Table 9: Summary of calculated principal shear stresses for load case 3.

	Principal shear stress (MPa)	**Stress rupture (MPa)**	**Safety coefficient**
Bulkhead biaxial	24	300	112.5
Panel floor biaxial	0	300	-
Keel UD	8	1000	125
Deck line UD	4	1000	250
Deck Biaxal	28	300	10.7
Hull Biaxal	9	300	33.3

Note that the floor panel in Table 9 shows no shear stresses. The reason is that there is no floor panel before bulkhead number four, and hence, the structural rigidity of this part of the float is only made by the bulkhead. In addition, the maximum shear stress occurs in the deck of the float, in front of the loaded area. It is explained by the presence of a bulkhead just in the middle of the back part of the float. This bulkhead supports most of the shear stresses given by the load case, and consequently, low shear stresses are found in the back part of the float.

Summary of study 1

By comparison of the three load cases, the first load case that simulates the float going through a wave was deemed to be the worst. Hence, it was used in the following study in Section 5.3.2.

The results from load cases 2 and 3 showed that the structural behaviour and characteristics of the float fulfilled the targets, and therefore, the laminate scantling for these parts did not have to be further optimised except for if the results will be very different when the material data from completed materials testing are used instead.

5.3.2. STUDY 2 - LOAD CASE 1 AND PRESSURE LOAD

In this study, the main influence and contribution of the unidirectional fibres regarding the structural resistance of the float was investigated. According to the draping plan made by the architects of the floats, the keel and deck line (unidirectional areas) were divided into mesh zones with varying properties of the elements; i.e. the number of UD plies varies along the length of the float according to Fig. 20. The largest number of layers is close to the front arm because it has to carry large amount of loads and also transfer loads between the float and the main hull. Moreover, the non-homogeneous scantling follow the stress localisation which occurs for e.g. swell load case 1 where the large stresses occurred near the bulkhead but low stresses occurred in front of the float. Thus, additional unidirectional layers are required around the bulkhead to support the stresses.

Study 2 was divided into two parts:

- In the first part, the FE model is remeshed to have properties with varying laminate scantling in the unidirectional zone (deck line and keel) according to Fig. 20. The structural analysis is carried out using swell load case 1 which is described in the former Section 5.3.1 as the worst load case of the three swell load cases tested. The objective was to obtain more realistic stress results and also to study the influence of the scantling of unidirectional fibres in deck line and keel areas in comparison with the calculation presented in Section 5.3.1 using the same load case.
- In the second part, a pressure load was applied on the front hull part of the float in addition to load case 1. The pressure load was applied as a uniformly distributed load on the front hull part of the float. The objective was to investigate the structural resistance and behaviour of the float structure under a superposed pressure load. If the results show that the safety coefficient is too low, the scantling of the current design of the composite should be updated to resist to the water pressure load.

Figure 33 presents the calculated displacement of the float for load case 1. The maximum displacement was calculated to 58 mm. Figure 34 shows an example of the principal stress for the same load case, and Table 10 presents the principal stresses in different parts of the float.

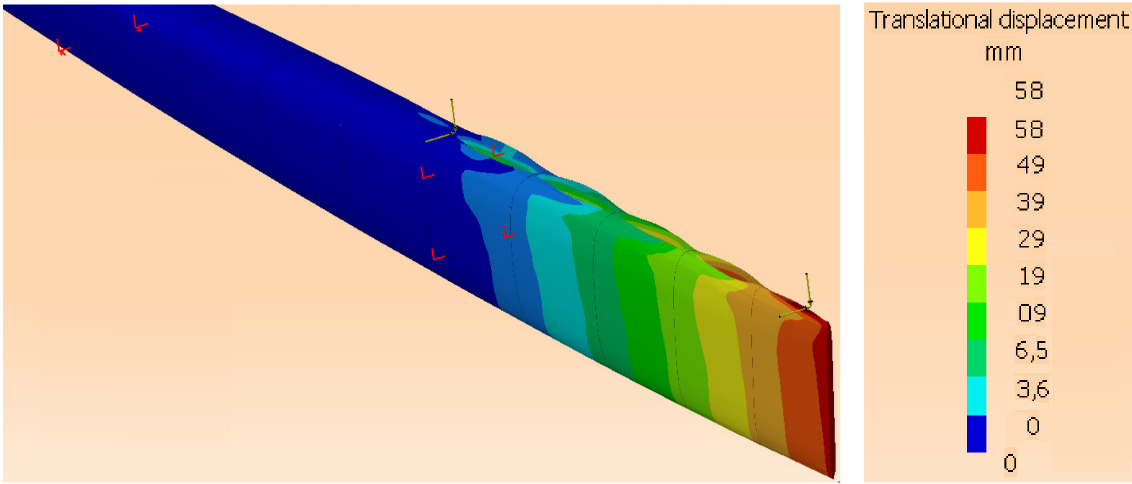

Fig. 33: Calculated displacement of the float for load case 1.

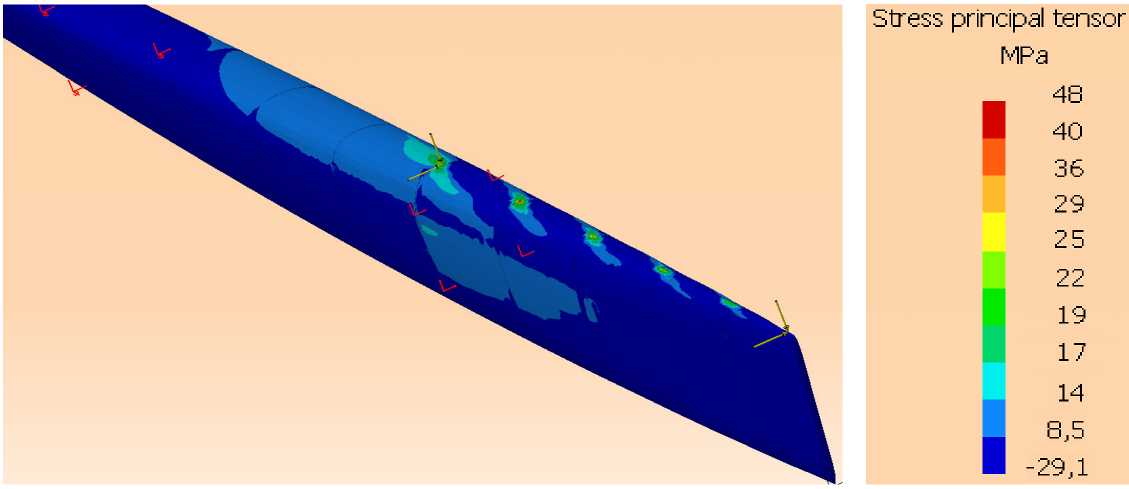

Fig. 34: Example of calculated principal stress of the float for load case 1.

Table 10: Summary of calculated principal shear stresses for load case 1.

	Principal stress (MPa)	Stress rupture (MPa)	Safety coefficient
Bulkhead biaxial	85	300	3.5
Panel floor biaxial	28	300	10.7
Keel UD	156	1000	6.4
Deck line UD	132	1000	7.6
Deck Biaxal	110	300	2.7
Hull Biaxal	48	300	6.3

A comparison of the results between Table 7 and Table 10, i.e. the results in study 1 versus study 2 for the same load case, shows that the stresses in the latter study is lower. Hence, unidirectional fibres in the keel and deck line areas can carry larger loads and the scantling was for this reason considered sufficient. Consequently, the safety coefficient is higher for the structural design in study 2.

In the second part of this study, a pressure load was applied on the planking of the float. The pressure load distribution was 1 tonnes/m^2 which is an amplified load used for this study only and may never occur during sailing conditions. However, it was used here to investigate the structural response due to an extreme overload in order to see if the current composite scantling design is sufficiently strong and can resist damage.

Figure 35 presents the principal stress results in the biaxial fibre of the float. The maximum principal stress that occurs is 244 MPa which is less than the limiting stress of rupture which is 300 MPa; hence, the safety coefficient is 1.2. Despite the low value of the safety coefficient, the structural design was deemed satisfactory due to the fact that the pressure load used in the current study was higher than what is normally used during structural analysis design procedures.

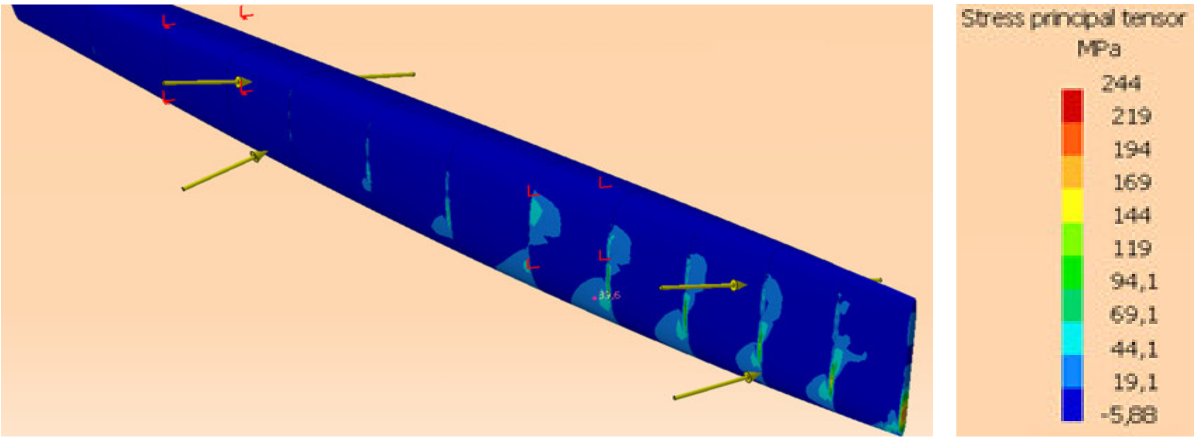

Fig. 35: Pressure load on the hull part of the float,

Summary of study 2

The structural analysis and calculations in study 2 show that the global behaviour and local strength of the float benefit from the current composite scantling design in comparison with the study 1 model.

The superposed pressure load analysis on the planking showed that the resistance of the structure was satisfactory even if the safety coefficient was 1.2. The load applied was higher than what may occur during sailing conditions and it will still survive this load without structural collapse.

6. FE MESH OF THE MULTIHULL RACING BOAT

This section describes the development of the FE mesh of the entire multihull racing boat. The FE model was divided into parts whose descriptions are commented on in the following sections:

- the main hull,
- representation of connections between the main hull, the arms and the floats,
- the traveller track connection and
- the rudder and the centre-board reinforcements.

Due to symmetry, one half of the multihull racing boat was meshed and thereafter “mirrored” to achieve a symmetric FE mesh of the sailing boat [7].

6.1. MAIN HULL

The main hull was meshed similar to the procedure for the floats: the hull was divided into zones which were given different properties depending on e.g. type of laminate scantling. In Fig. 36, the FE mesh of the UD deck line is shown with a variation of the UD fibre scantling along the length of the hull. Each of the different colours indicates a unique UD fibre scantling zone.

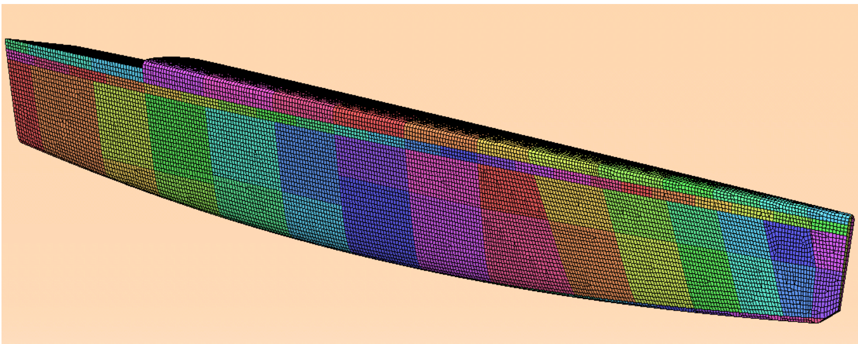

Fig. 36: One half of the FE mesh of the main hull. The variation in composite laminate scantling is shown by the different colours of the meshed areas.

6.2. CONNECTIONS BETWEEN THE MAIN HULL, THE ARMS AND THE FLOATS

The connection between an arm and a float is illustrated in Fig. 37. Both the back and front arms were connected to a float at a bulkhead and the mesh of the arms therefore had to be adapted to the mesh of the bulkheads. This representation of the connection is an established modelling technique in multihull structural analysis because, during a swell load case, the floats and main hull interact via the arms in a realistic way.

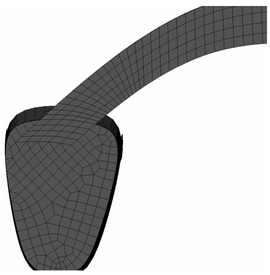

Fig. 37: Illustration of a mesh-connection between a float’s bulkhead and an arm.

The connections between the arms and the main hull were modelled similarly as the float and arm connections: both arms were connected to a bulkhead and the meshes were adjusted accordingly, see Fig. 38.

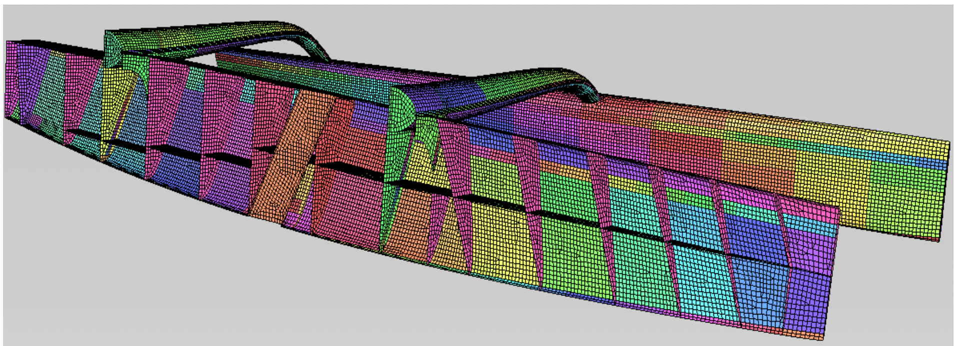

Fig. 38: Finite element mesh of the connection between the arms and the main hull.

In the design of the multihull, the areas near the connection between an arm and the main hull are strengthened using a “webbing” technique: unidirectional (UD) fibres are rolled up around the arms to make a more rigid fixture of the arms to the main hull structure. By doing that, the multihull structure can sustain the loads transmitted by the arms from the float to the main structure. Figure 39 illustrates the numerical representation of the reinforcement near the arm and main hull structure connections called webbing.

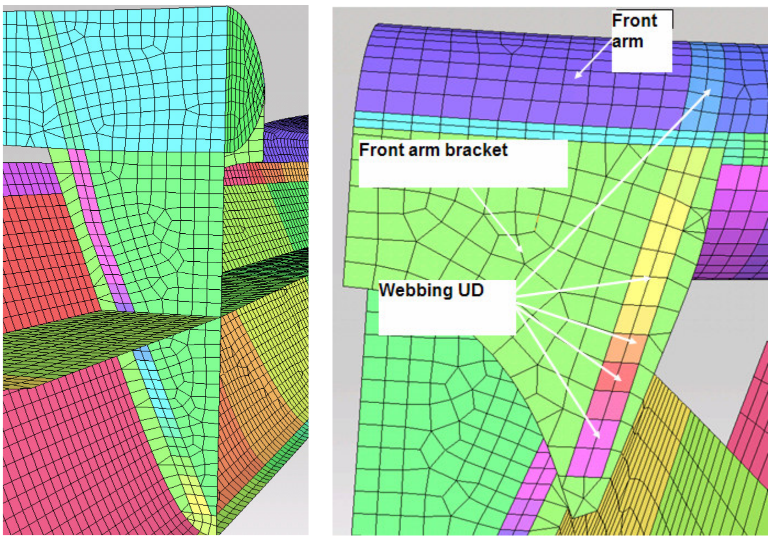

Fig. 39: Webbing: reinforcement using UD fibres around the arms and bulkheads of the main hull structure.

6.3. THE TRAVELLER TRACK CONNECTION

The traveller track is illustrated in Fig. 40. One of its functions is to transfer the loads from the main sail to the multihull structures, in this case in three positions in the figure.

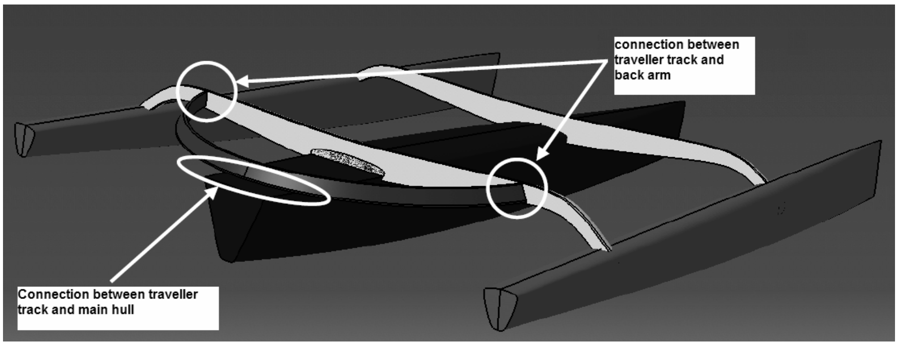

Fig. 40: The traveller track and its connections with the multihull structure.

The design of the mechanical joint is shown in Fig. 41. It shows one part that has to be attached to the hull part near a bulkhead, where locally the structure has to be reinforced, and another part that can be attached to the traveller track using a screw joint. It should be mentioned that the part of the joint connected to the hull structure needs to be further investigated to ensure that composite scantling reinforcement is properly designed and dimensioned to resist damage [7].

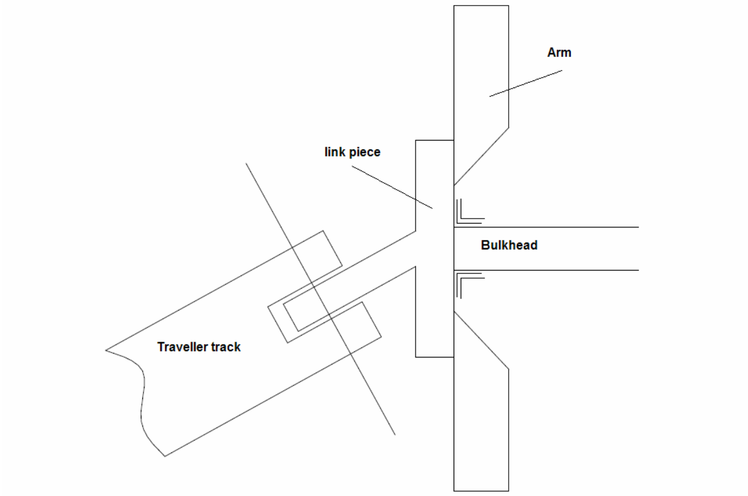

Fig. 41: Schematic of the mechanical joint of the traveller track to the hull structure.

In the FE model, this joint was represented by a virtual knuckle in the CATIA geometry model, see Fig. 42. In the FE model, it was represented by master and slave node definitions using rigid beam connections, see Fig. 43.

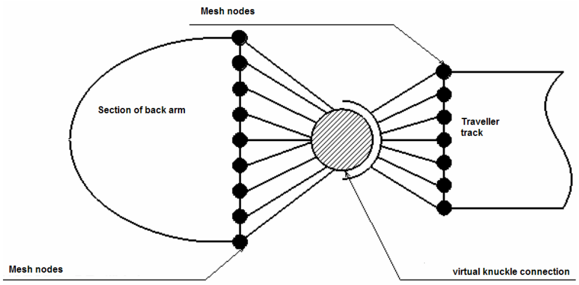

Fig. 42: Virtual knuckle connection as represented in the CATIA model [7].

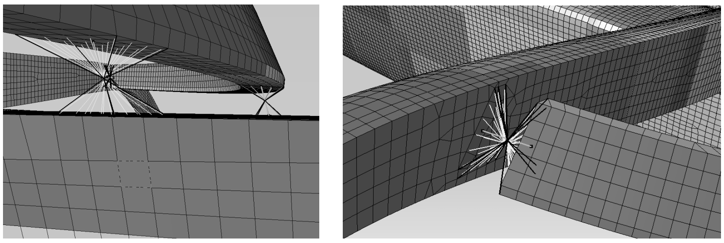

Fig. 43: Representation of the “knuckle” in the FE model using master and slave node connections and rigid beam elements.

6.4. RUDDER AND CENTRE-BOARD REINFORCEMENTS

The rudder and centre-board are essential parts of a multihull racing boat. They have to sustain very large loads sometimes, both static and dynamic, and therefore, special consideration to their areas of connections to the mainhull is required. The designers of the Tri80 multihull have proposed special reinforcements to ensure that the rudder and centre-board reinforcements can carry load impacts from e.g. bumping into objects like containers, wood, or whales. The FE model of the mainhull near these areas was created considering the architects’ suggestions, see Fig. 44.

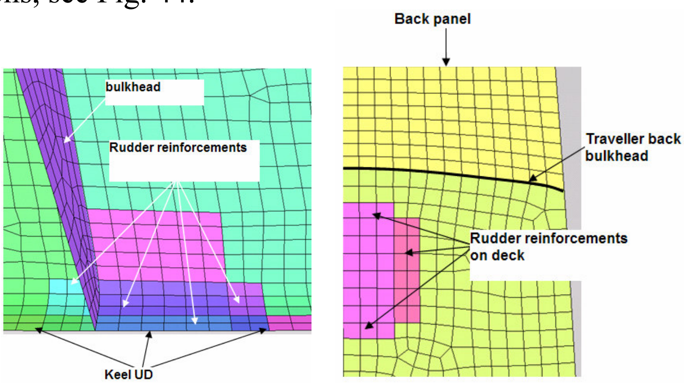

Fig. 44: FE model representation of the reinforced zones near the rudder

6.5. FINAL MESH OF THE MULTIHULL RACING BOAT

Due to symmetry conditions, only half of the CATIA geometry model was meshed. The full mesh of the multihull racing boat was obtained by mirroring [7] of the meshed part around the length axis of the mainhull, see Fig. 45. The FE mesh in the figure shows the parts that were completed within the current thesis work and which have been reported in the previous sections.

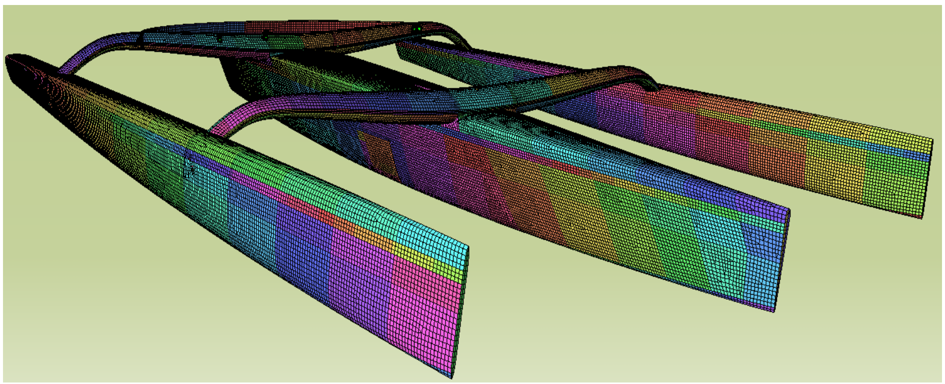

Fig. 45 Finite element mesh of the mainhull structure.

7. DISCUSSION AND FUTURE WORK

All of the mechanical tests that were described in Section 2 were not completed during the time the current thesis work was carried out. Therefore, the structural analyses presented show the characteristics of the multihull racing boat based on mechanical properties taken from similar investigations and materials. The actual values for the current design and composite materials can only be determined once the planned mechanical tests are completed. Nevertheless, the results presented show that the safety factors against failure are acceptable and they are anticipated to not change too a large extent even if the values from completed mechanical testing are used instead.

Large effort was spent in this thesis work to develop the finite element model of the multihull racing boat. This is a complicated task both from a numerical modelling perspective (meshing) as from a material representation perspective (material properties). Regarding composite scantling its influence and modelling representation was quantified by FE calculations. Still, there may be some more work to do to further optimise the structure.

The FE model developed and presented this far within the Tri80 project shows satisfying results, using the anticipated composite material characteristics, with respect to first virtual prototype design model. The scantling plans provided by the designers/architects of the multihull were verified but can be further optimised when the final set-up of material data for the composite material are available from the mechanical tests.

In future work, it is strongly suggested to benchmark the FE software that is going to be used. In this investigation, CATIA and NASTRAN were compared. In the benchmark between these softwares, a lot of lessons were learnt how results are presented and should be interpreted. Additionally, in further optimisation of the structures, the position of unidirectional fibres in the hulls should be studied to decrease the sometimes high shear stresses which occur locally.

8. CONCLUSIONS

This investigation presents the initial structural analyses of a multihull racing boat. It incorporates the descriptions of the mechanical tests which are necessary to determine the material characteristics of composite materials and also the numerical modelling of the global structure of the multihull. The work was carried out in the Tri80 project in France, which unfortunately could not be completed due to lack of funding. Hence, the planned work of this thesis had to be limited.

The major contribution of this work to the Tri80 project came from the FE modelling of the multihull structure. A global FE model of the structure was established with necessary connections properly modelled with respect to their functions. Detailed structural analyses of a float, using material properties for a similar type of composite material as the intended design, were presented. Three swell load cases were compared for two structural design solutions of the floats: homogeneous spacing between scantlings and scantling distance as proposed by the multihull designers. The FE calculations showed that homogeneous scantling of unidirectional fibre in the float resulted in higher critical stresses in contrast to when the number of unidirectional plies was varied along the length of the float. Hence, the latter is recommended for use in future designs of multihulls.

.

9. REFERENCES

[1] D. Presles and D. Paulet (1998). Architecture Navale, connaissance pratique. Edition de la villette 1998 (In French). http://perso.orange.fr/c.paulet/archi/. (2007-10-17).

[2] Dassault Systems (2007). Guide for CATIA ver 5: http://www.3ds.com/fr/. (2007-10-17).

[3] MSC NASTRAN (2007). MSC Software: http://www.mscsoftware.com/. (2007-10-17).

[4] D. Gay (1997). Matériaux composites (In French). Hermes, Paris, France.

[5] P. Berney (1992). Les préimprégnés dans le nautisme (In French). In: *La construction navale en composites - IFREMER, Arles tic colloques no.15, communication no.11*. December 7-9, 1992: Paris, France.

[6] Gurit (2007). Marine handbook: http://www.gurit.com/. (2007-10-17).

[7] R. Larsson (2004). A course on computational solid mechanics. Report U70, Department of Applied Mechanics, Chalmers University of Technology, Göteborg, Sweden.

[8] N. Ottosen and H. Petersson (1992). Introduction to the finite element method. Prentice-Hall, London, U.K.